

Finite Element Analysis of the Mechanical Behavior of Mitered Steel Pipe Elbows under Bending and Pressure

Spyros A. Karamanos¹; Konstantinos Antoniou²; Brent Keil³; and Robert J. Card⁴

¹Univ. of Thessaly, Volos, Greece. E-mail: skara@mie.uth.gr

²Univ. of Thessaly, Volos, Greece. E-mail: konsanto@uth.gr

³Northwest Pipe Company, Vancouver, WA. E-mail: BKEIL@nwpipe.com

⁴Lockwood, Andrews & Newnam, Inc., Houston, TX. E-mail: RJCard@lan-inc.com

Abstract

Using finite element simulation tools, which account for both geometric and material nonlinearities, the bending capacity of mitered steel pipe bends is investigated. First, numerical results are reported on the elastic behaviour of two steel typical grade 40 steel mitered elbows with D/t values equal to 192 and 240, with the purpose of calculating flexibility and stress intensity factors. Furthermore, the elastic-plastic response of the two bends is also examined towards identifying their ultimate capacity and the corresponding mode of failure. Internal pressure effects on the structural response are also examined. The present paper addresses some important features of mitered steel pipe elbow response that may arise in geohazard areas, towards safeguarding the structural integrity of steel water pipelines subjected to severe ground-induced actions.

INTRODUCTION

The present paper is motivated by the need for determining the deformation capacity of welded steel pipelines for water transmission, constructed in geohazard areas. In such areas, e.g. areas with significant seismic activity, the pipeline can be subjected to severe permanent ground deformations, resulting from fault rupture, liquefaction-induced lateral spreading and subsidence, or landslide action. Under those extreme loading conditions, the pipe deforms well beyond the stress limits associated with normal operating conditions, whereas the structural performance of welded joints constitutes a key issue for pipeline structural integrity (Lund, 1996; O' Rourke and Bonneau, 2007). In such geohazard areas, the main action on the pipeline is bending loading.

Previous work on the structural performance of steel pipe elbows has mainly focused on “smooth” elbows, fabricated mainly through “induction bending”, which are widely used in industrial piping applications (refineries, chemical industries or nuclear plants). This research has shown that smooth elbows exhibit a unique structural behaviour under structural loading, characterized by significant flexibility and stress concentration, and therefore, they may constitute “weak spots” of the piping system in the course of a severe seismic event. For an overview of smooth elbow mechanical behaviour, the reader is referred to the review paper by Karamanos (2016). On the other hand, the response of mitered elbows has received much less attention. It is worth mentioning the experimental-analytical work presented by Gresnigt (2002), as well as the review paper by Wood (2008), which offers an overview of the mechanical behaviour of mitered bends under various loading conditions.

Mitered elbows are widely used in large-diameter steel pipelines for water transmission. In the USA, they are manufactured according to the provisions of AWWA C208 standard, whereas their design follows the provisions of AWWA M11. They are also employed in several pipeline and industrial piping applications associated with relatively low levels of operational pressure, as alternative to smooth elbows whenever the use of latter may not be feasible or cost-effective. Figure 1 shows the configuration of typical mitered pipe bends used for water transmission pipelines in the US. Furthermore, Figure 2 shows the bends from a water transmission pipeline overseas; it is interesting to note that the elbow segments are connected on site.

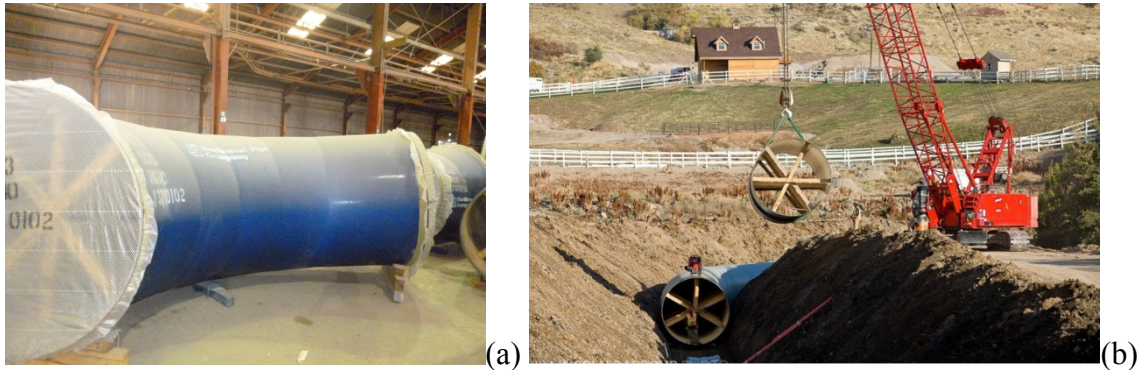


Figure 1. Mitered steel pipe bends; (a) bend manufactured in Northwest Pipe Co., Fort-Worth plant; (b) mitered bend in a buried steel water pipeline under construction.

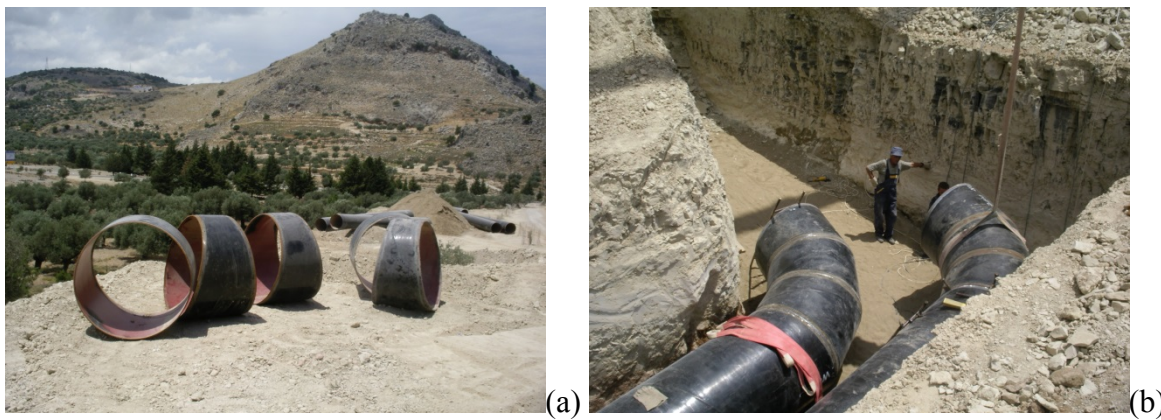


Figure 2. Mitered steel pipe bends, used in a 48-inch-diameter water transmission pipeline in Rhodes, Greece, a high-seismicity area; (a) pipe bend segments before welding; (b) pipe bends during pipeline construction.

The present study reports a finite element simulation of the structural performance of large-diameter mitered pipe bends subjected to bending loading conditions, in the presence of internal pressure. Special attention is given on the geometry of mitered bends, where the connection between adjacent parts causes concentration of stress and deformation. Therefore, this geometric discontinuity results in localization of stress and deformation at the connection between two adjacent parts, and may differentiate substantially the response of mitered elbows from the response of smooth elbows, in terms of their structural capacity under bending and pressure.

In the present simulation, the elbow is considered together with two straight pipe segments, connected at each side of the elbow, so that a realistic representation of elbow response within the pipeline is modelled. The elbow and the two straight parts are modelled with nonlinear finite elements, so that a “numerical testing laboratory” is developed, capable of describing pipe deformation in a rigorous, reliable, yet cost effective manner.

Numerical results are presented for two 90-degree mitered steel pipe bends, with diameter-to-thickness ratio values between 192 and 240, subjected to longitudinal bending and internal pressure. The configuration of both elbows is chosen according to the AWWA C208 standard. The elbows are subjected to in-plane bending (opening and closing bending moments), in the presence of internal pressure up to 50% of yield pressure; elastic response is considered first, focusing on flexibility and stress intensity, followed by elastic-plastic analysis associated with ultimate capacity and collapse of the bends.

ASPECTS OF ELBOW STRUCTURAL BEHAVIOR

The mechanical behaviour of pipe elbows is quite unique. Compared with straight pipe segments, it is significantly more flexible, it is associated with significantly higher stresses and strains and with very pronounced cross-sectional deformation, referred to as “cross-sectional ovalization”. Because of their flexibility, they are widely used in industrial piping applications, mainly because they can accommodate thermal expansions and absorb other externally-induced loading. Nevertheless, they are considered as critical components for the structural integrity of piping systems. For the case of extreme loading conditions, their mechanical response is characterized by a biaxial state of stress and strain (Figure 3), which may lead to pipe elbow failure, in a mode quite different than the one expected in straight pipes.

The early analytical work of Von Karman (1911) was pioneering in understanding the particular mechanical behavior of smooth (not mitered) pipe bends. Von Karman, employed a simple two-dimensional formulation that couples longitudinal deformation due to bending, with hoop deformation due to ovalization, and considers a simple doubly-symmetric trigonometric function for the radial displacement of arbitrary point of the elbow cross-section w (Figure 3). A more enhanced energy formulation has been proposed by Rodabaugh and George (1957) to describe in more detail the mechanical behavior of elastic elbows, including the effects of internal pressure, as a generalization of the Von Karman (1911) solution. The work of Rodabaugh and George (1957) has been the basis for the development of the ASME B31 flexibility and stress intensity factors, presented and discussed in the next section.

Despite the extensive and continuing research on the mechanical behaviour of smooth elbows (mainly because of their applications in the oil & gas and the nuclear sector), the behaviour of mitered bends has received less attention. The work by Rodabaugh (1975) has been the basis for the design rules in ASME B31. Previous works (Gresnigt, 2002; Wood, 2008) have demonstrated that there exist several similarities between the structural response of mitered elbows and the response of smooth elbows; mitered elbows exhibit both cross-sectional ovalization and stress intensity, mainly at the corners between the adjacent parts. Furthermore, the presence of corners may accentuate those local phenomena, causing failure of the elbow.

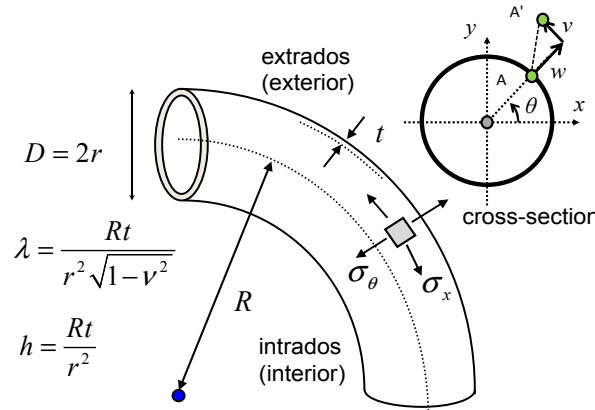


Figure 3. Response of a smooth pipe elbow subjected to in-plane closing bending moments (Karamanos, 2016).

DESIGN PROVISIONS FOR MITERED BENDS

Design provisions for both smooth and mitered elbows from two acclaimed design specifications are briefly presented in this paragraph. They are both based on elastic elbow analysis. The ASME provisions refer to bending loading conditions, in the framework of pipe stress flexibility analysis, whereas the AWWA provisions focus only on pressure loading conditions.

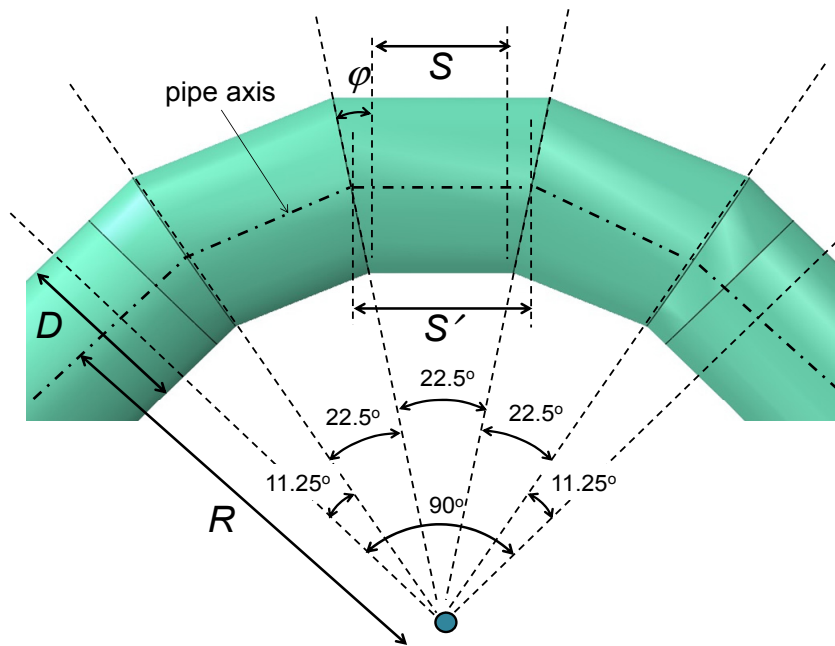


Figure 4. Geometry of mitered pipe bends, according to AWWA C208 specification.

ASME B31

ASME B31 consists of a series of standards for the design and construction of piping and pipeline systems. In several of those standards [B31.1 for power piping, B31.3 for process piping, B31.4 for liquid pipelines, B31.8 for gas pipelines], flexibility and stress intensity

factors are proposed for elbow design (both smooth and mitered) in terms of their geometry and the level of pressure. They are based on the papers by Rodabaugh and George (1957) for smooth bends, and Rodabaugh (1975) for mitered bends. More specifically, the following factors are proposed:

Flexibility factors

$$\text{Smooth elbows:} \quad k = 1.65/h \quad (1)$$

$$\text{Mitered elbows:} \quad k = 1.52/h^{5/6} \quad (2)$$

Stress intensity factor (in-plane bending):

$$\text{Smooth and mitered elbows:} \quad i = 0.90/h^{2/3} \quad (3)$$

In the above equations, for smooth elbows: $h = Rt/r^2$, whereas for mitered elbows: $h = 0.5(tS'/r^2) \cot \phi$ (see Figure 3 and Figure 4). The flexibility factor k should divide the nominal bending stiffness of the pipe, whereas the stress intensity factor i should multiply the nominal stress, calculated through standard mechanics of materials. The above factors can be found in ASME B31.4, Table 402.1-1, and refer to zero internal pressure. In the presence of internal pressure p , a reduction factors is proposed as follows, to account for its stiffening effect:

Flexibility

$$1 + 6 \frac{p}{E} \left(\frac{r}{t} \right)^{7/3} \left(\frac{R}{r} \right)^{1/3} \quad (4)$$

Stress intensity

$$1 + 3.25 \frac{p}{E} \left(\frac{r}{t} \right)^{5/2} \left(\frac{R}{r} \right)^{2/3} \quad (5)$$

These pressure reduction factors should divide the corresponding flexibility and stress intensity factors. It should be noted that all the above formulae have been based on elastic analysis, and are used extensively in the design of pipe elbows. However, the case of extreme loading, associated with severe plastic deformation, and the corresponding failure modes have not been addressed in those provisions.

AWWA M11

In M11 design manual, the issue of pressure loading on mitered bends is addressed. In particular, the following equation is proposed, for determining pipe elbow thickness t_e in terms

of internal pressure level, allowable stress σ_w and elbow geometry (AWWA M11, Chapter 9, equation 9-3):

$$t_e = \frac{pD}{2\sigma_w} \left(1 + \frac{D}{3R - 1.5D} \right) \quad (6)$$

Comparing this equation with the standard Barlow equation for pipe wall thickness calculation, the term in the parenthesis on the right-hand side of equation (6) represents the increase of stress due to elbow geometry. Assuming elbow radius R equal to 2.5 times the pipe diameter D , one may readily obtain a 17% increase of thickness in the elbow, with respect to straight pipe, which means, equivalently, a 17% increase of local stress for a given value of pipe bend thickness. However, no provisions exist for the case of structural loading of mitered elbows.

DESCRIPTION OF MITERED BENDS EXAMINED

Two 90-degree pipe bends ($\Delta = 90^\circ$) with different diameter-to-thickness ratio D/t are examined in the present study. The first pipe, denoted as “pipe I”, has a 48-inch diameter and 0.25-inch wall thickness (D/t equal to 192), whereas the second pipe, denoted as “pipe II”, is a 77.625-inch-diameter pipe and 0.323-inch wall thickness (D/t equal to 240). Both mitered bends have a bend radius R equal to 2.5 times the pipe diameter, and 5 segments, according to AWWA C208, as shown in Figure 4. In each case, the bend is connected to two straight pipe parts, each one of length equal to five pipe diameters. In the following, the assembly of the bend with the two straight pipe segments is referred to as “pipe specimen”. The two ends of the pipe specimen are capped, so that internal pressure can be applied.

The material of both bends is ASTM 1018 grade 40 steel, and the stress-strain curve is shown in Figure 5. The yield stress is 303 MPa (43,900 psi), there is a plastic plateau up to 1.5% of strain, and subsequently, strain hardening occurs, with a plastic modulus equal to approximately 1/500 of Young’s modulus. This material curve has also been employed in the analysis of welded lap joints in Karamanos *et al.* (2015).

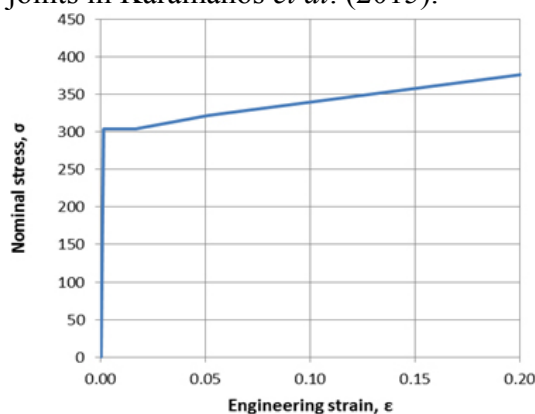


Figure 5. Stress-strain curve of ASTM 1018 grade 40 steel used in the present analysis; yield stress is equal to 303 MPa [43,900 psi].

NUMERICAL MODELLING

Three-dimensional numerical models are employed to simulate the mechanical behavior of the bend. The models are developed in the software ABAQUS/Standard, an implicit finite

element program. The pipe specimen (i.e. all parts of the elbow and the straight pipe segments) are modelled with three-dimensional nonlinear four-node reduced-integration shell elements, which have been quite efficient in simulating buckling and post-buckling response of thin-walled cylindrical members (Vasilikis *et al.*, 2014; Karamanos *et al.*, 2015). Those elements can account for geometric nonlinearities, such as large deformations and local buckling, as well as the nonlinear (inelastic) behaviour of steel pipe material well beyond the elastic regime.

The numerical models do not account for any symmetry, despite the fact that the elbow geometry and the deformation are initially symmetric with respect to both the plane of bending and the middle section of the elbow. However, upon occurrence of local buckling, the corresponding buckled shape of the bend may not be necessarily symmetric, and therefore, full three-dimensional models should be considered.

The model contains a dense mesh in the area of the mitered elbow, where the element size is equal to $1/57$ of the pipe diameter in both the axial and the circumferential direction. It is noted that, from shell buckling theory, a good estimate for the half-wave length in the axial direction of the pipe can be obtained from $1.3\sqrt{Dt}$. This means that for a pipe with D/t equal to 240, five (5) elements are contained within each half-wavelength, a number which is considered satisfactory for the purposes of the present analysis. A coarser mesh is considered for the straight pipe segments outside the elbow.

At the two end sections of the pipe specimen model, two “fictitious” nodes are introduced on the pipe axis, connected to the nodes of the end-section with appropriate kinematic conditions, employing the “kinematic coupling” feature in ABAQUS. The pipe specimen model is considered simply-supported in those two ends, and bending is applied with either two opposite bending moments or two opposite forces at the end nodes. The analysis is nonlinear through a step-by-step (incremental) displacement-control procedure.

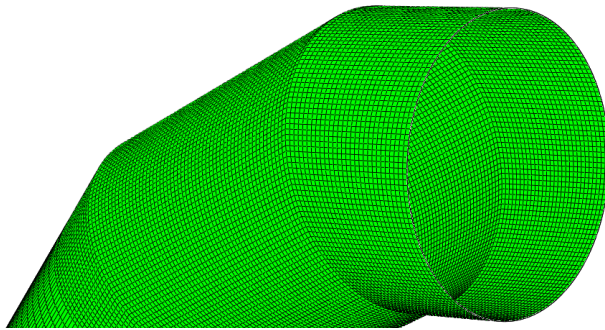


Figure 6. Finite element mesh of a mitered bend (half elbow is shown for visualization purposes).

NUMERICAL RESULTS

Two types of numerical analysis are performed. The first, referred to as “elastic analysis”, is associated with the determination of elbow flexibility and stress intensity. The second type of analysis, referred to as “elastic-plastic analysis”, is aimed at determining the maximum load and bending moment sustained by the elbow and the corresponding mode of failure.

Elastic analysis

The flexibility factor of the mitered elbow is calculated in accordance with the corresponding definition introduced by the ASME B31 code. In the course of the present study,

assuming elastic material behavior, and considering geometrically nonlinear behavior, two opposite bending moments are applied at the two specimen ends (

Figure 7a) so that the corresponding relative rotation θ of the two end sections A and B in

Figure 8a is calculated. Furthermore, the same bending moments are applied at the ends of a straight pipe of length equal to the length of the entire specimen and the corresponding relative rotation θ' of sections A' and B' in

Figure 8b is calculated. Finally, these bending moments are applied on a straight pipe of length equal to the length of the straight parts of the specimen, and the corresponding relative rotation θ_s of the two end sections A_s and B_s in

Figure 8c is calculated. The flexibility factor is equal to the ratio:

$$k = \frac{\theta - \theta_s}{\theta' - \theta_s} \quad (7)$$

Equation (7) for calculating the flexibility factor is in accordance with the definition of ASME B31; subtracting the rotation of the straight pipe segments θ_s , the effect of the bend on flexibility is determined. The values for this flexibility factor for the elbows under consideration are depicted in Table 1 and compared with the flexibility factors calculated according to the ASME B31 provisions. For both elbows, a small bending moment equal to 3.5% of nominal plastic moment $M_p = \sigma_y D^2 t$ is considered in the analysis. Furthermore, the corresponding factors calculated for a “fictitious smooth” bend are reported in Table 1, shown in

Figure 7b. An appropriate numerical finite element model has also been developed for the analysis of the smooth elbow. This smooth bend is assumed to have the cross-sectional properties of the pipes under consideration and a bend radius R equal to 2.5 the pipe diameter. It is referred to as “fictitious” in the sense that it may not be feasible to construct such a smooth elbow with the dimensions under consideration in a practical application, but its analysis may be used for comparison purposes. The results show that the flexibility factors computed numerically for mitered bends are higher than the predictions from the ASME provisions. Furthermore, the values of flexibility factor for mitered bends are quite close to those computed for smooth bends.

In addition to the flexibility factor, the stresses developed in the mitered elbow are of particular interest. The numerical results show that the critical sections of the mitered elbow in terms of stresses are located at the corners connecting the adjacent parts, whereas for the smooth elbow, the critical section is the middle elbow section. The distribution of longitudinal stress and hoop stress at these critical cross-sections are shown in Figure 9 and Figure 10 for opening and closing bending moments, for zero pressure and for pressure 50% of the nominal yield pressure ($p_y = 2\sigma_y t/D$). It is interesting to note that the distribution of stresses in both mitered and smooth elbows is substantially different than the linear distribution calculated using Mechanics of Materials, corresponding to the one of a straight pipe of the same cross-sectional geometry. Furthermore, the maximum stresses developed in both mitered and smooth elbows are significantly higher than the one corresponding to the straight pipe.

In order to quantify the depicted stress distributions, the so-called “stress intensity factor” is introduced, also adopted by the ASME B31 code. It is defined as the ratio of the maximum

stress in the elbow σ_{max} , over the nominal stress σ_{nom} corresponding to a straight pipe with the same cross-section:

$$i = \sigma_{max} / \sigma_{nom} \tag{8}$$

In equation (8), the nominal stress σ_{nom} can be calculated from Mechanics of Materials $\sigma_{nom} = M / (\pi r^2 t)$, and r is the radius of the pipe cross-section ($r = D/2$). The values of stress intensity factors are depicted in Table 2 for mitered elbows I and II respectively. The results show that the value of the stress intensity factor reduces significantly in the presence of internal pressure, mainly because of the stabilizing effect of pressure that reduces cross-sectional ovalization significantly.

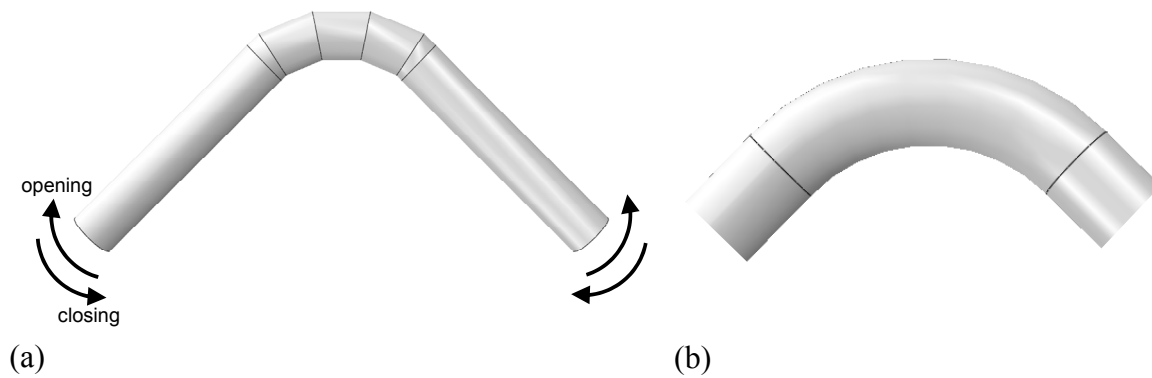


Figure 7. (a) Loading pattern for elastic analysis of mitered elbows; opening and closing bending moments; (b) “fictitious smooth” elbow, used for comparison purposes.

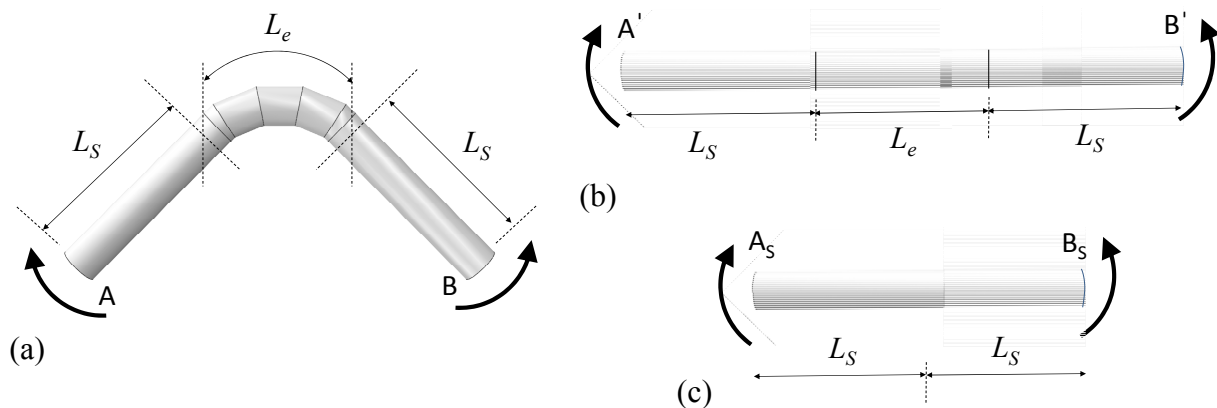


Figure 8. (a) Bending of elbow specimen; (b) bending of straight pipe with length equal to elbow specimen length; (c) bending of straight specimen part.

Elastic-plastic behavior and ultimate strength

For each case, the load-deformation relationship is determined for the loading pattern shown in Figure 11. The load-displacement curves are shown in Figure 12 and Figure 13. In all cases, the analysis shows that local buckling (bulging) and the subsequent folding due to excessive compression at the wall of the elbow is the failure mode. Nevertheless, the load-displacement diagrams depicted in Figure 12 and Figure 13 may not be valid beyond a certain point, because local strains may exceed a certain threshold that corresponds to local failure due to pipe wall fracture. Determining this strain threshold value may not be a trivial issue. Conservatively, based on pipeline strain-based design concepts, developed for hydrocarbon pipelines, this threshold value of strain may be taken equal to 2%. Monitoring the evolution of local strains at the critical locations, this threshold criterion is indicated in the load-displacement diagrams with an arrow (\uparrow). Beyond that stage, pipeline integrity may be threaten because of pipe wall fracture. The deformed shapes of the mitered elbows under opening and closing bending moments, for zero pressure and for pressure equal to 50% of p_y are shown in Figure 14 and Figure 15.

Mitered Elbow I

p/p_y	opening	closing	ASME B31.8
0	26.45	31.87	18.04
0.3	7.99	8.67	5.97
0.5	5.94	6.11	4.12

Smooth Elbow I

p/p_y	opening	closing	ASME B31.8
0	29.19	32.85	32.13
0.3	8.13	8.46	10.63
0.5	6.01	6.16	7.35

Mitered Elbow II

p/p_y	opening	closing	ASME B31.8
0	37.55	37.82	21.77
0.3	8.42	8.54	5.84
0.5	6.16	6.21	3.92

Smooth Elbow II

p/p_y	opening	closing	ASME B31.8
0	37.96	39.10	40.26
0.3	8.52	8.62	9.10
0.5	6.18	6.23	6.01

Table 1: Flexibility factors for elbows I and II.

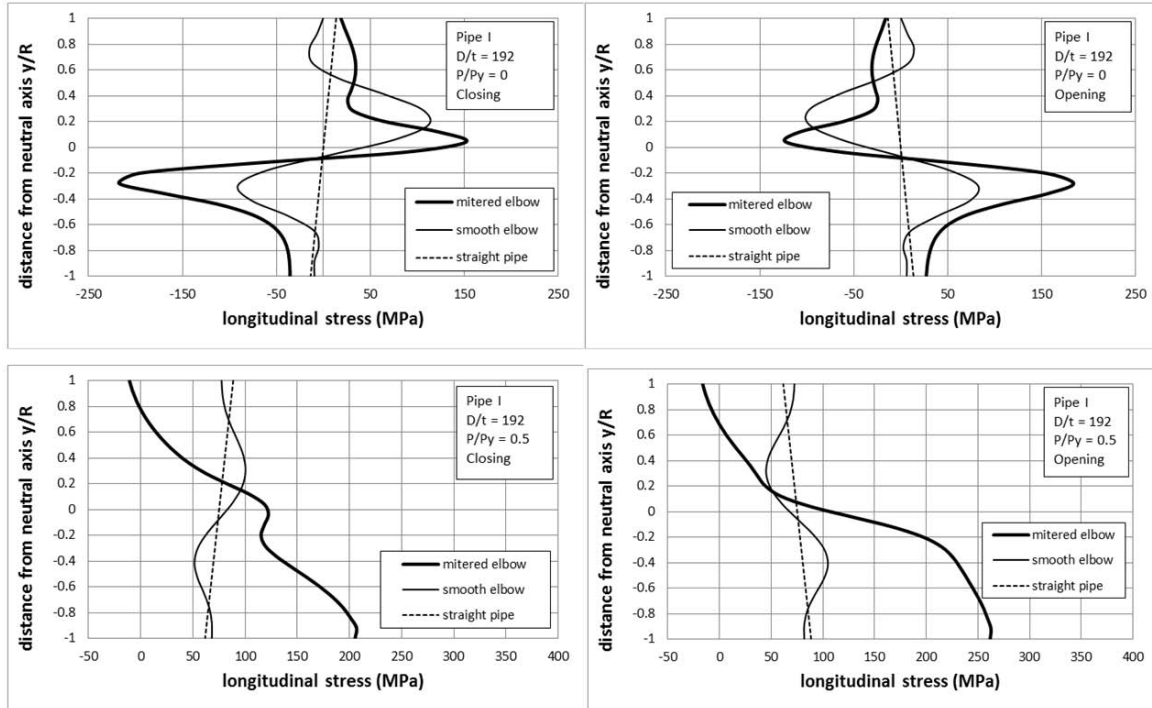


Figure 9. Distribution of axial stresses around the pipe cross-section for the mitered elbow (corner section), the “fictitious” smooth elbow (middle elbow section) and the straight pipe; pipe I, $D/t = 192$; closing and opening bending moments.

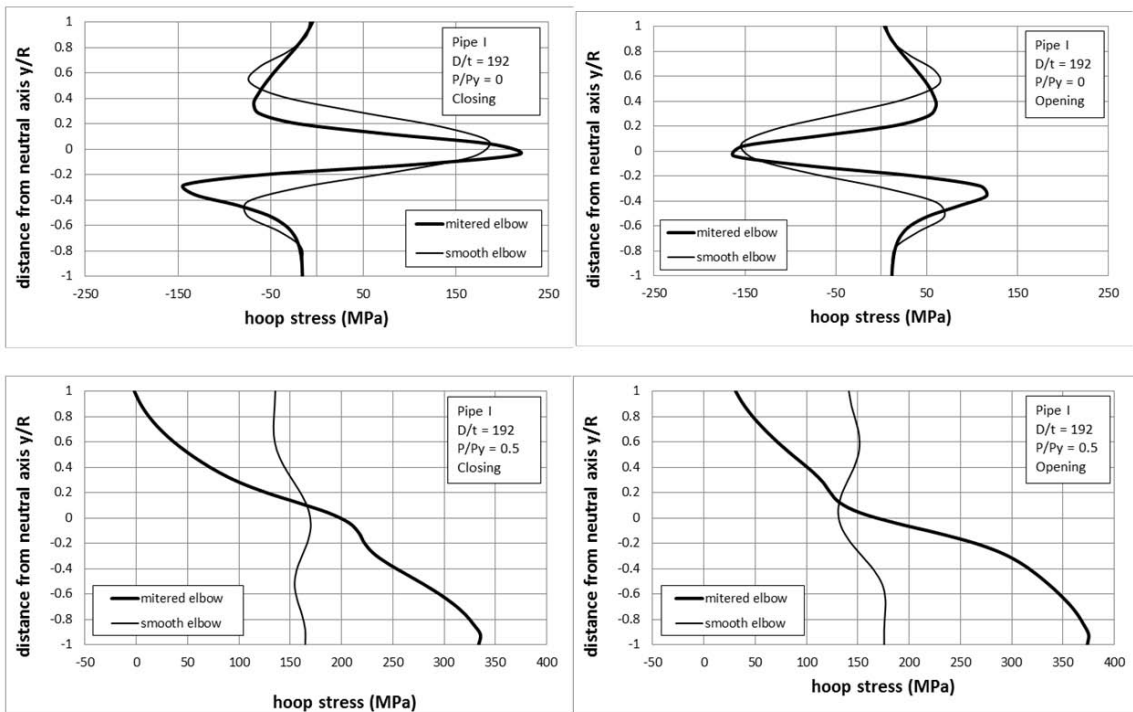


Figure 10. Distribution of hoop stresses around the pipe cross-section for the mitered elbow (corner section), and the “fictitious” smooth elbow (middle elbow section); pipe I, $D/t = 192$; closing and opening bending moments.

Mitered Elbow I – Axial Stresses

p/p_Y	opening	closing	ASME B31.8
0	13.54	16	6.51
0.3	1.97	2	1.31
0.5	2.04	2.05	0.85

Mitered Elbow I – Hoop Stresses

p/p_Y	Opening	Closing	ASME B31.8
0	11.92	16.09	6.51
0.3	1.34	1.36	1.31
0.5	1.44	1.47	0.85

Mitered Elbow II – Axial Stresses

p/p_Y	Opening	Closing	ASME B31.8
0	14.44	18.84	7.57
0.3	0.95	1.97	1.15
0.5	2.02	2.03	0.74

Mitered Elbow II – Hoop Stresses

p/p_Y	Opening	Closing	ASME B31.8
0	9.10	20.7	7.57
0.3	1.30	1.31	1.15
0.5	1.40	1.43	0.74

Table 2: Stress intensity factors for elbows I and II.



Figure 11. Loading pattern for elastic-plastic analysis of mitered elbows; opening and closing forces.

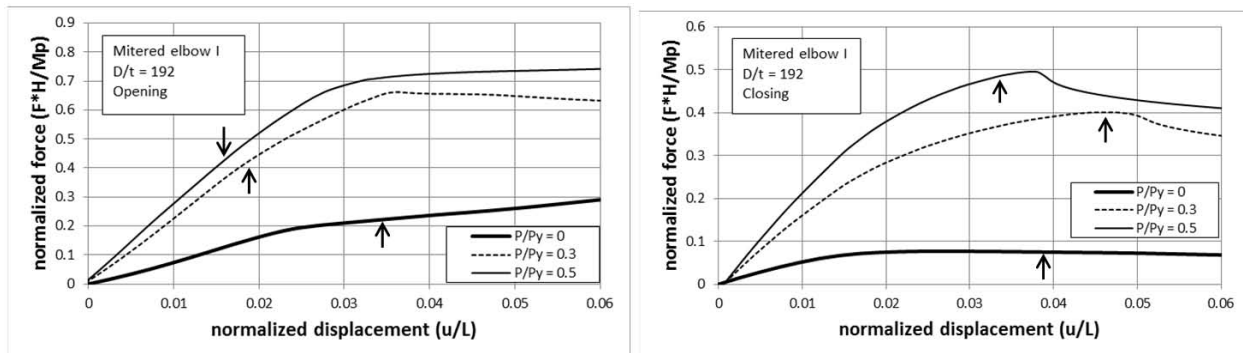


Figure 12. Load-displacement diagrams for elbow I; the arrows (\uparrow) indicate the stage at which local strain reaches the value of 2%; opening and closing bending moments.

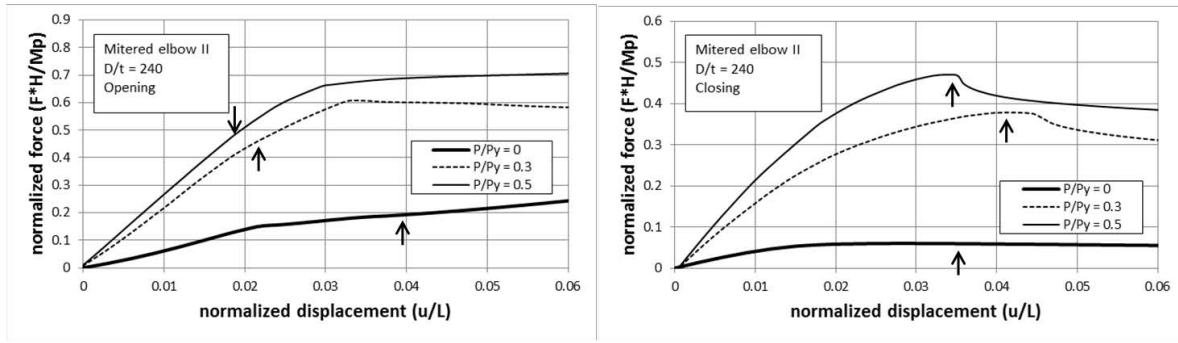


Figure 13. Load-displacement diagrams for elbow II; the arrows (\uparrow) indicate the stage at which local strain reaches the value of 2%; opening and closing bending moments.

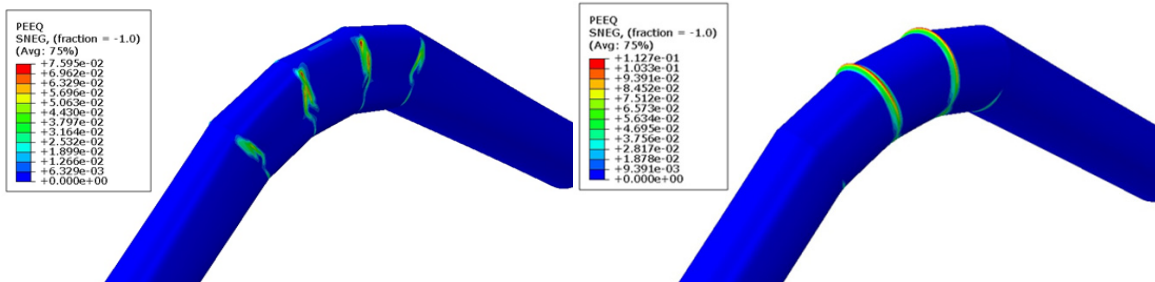


Figure 14. Deformed shapes of mitered elbows pipe II ($D/t = 240$); opening bending moments; (a) zero pressure and (b) pressure equal to 50% of p_y .

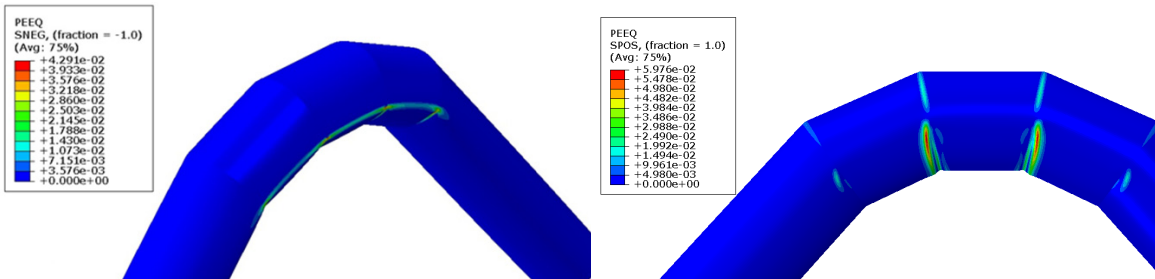


Figure 15. Deformed shapes of mitered elbows pipe II ($D/t = 240$); closing bending moments; (a) zero pressure and (b) pressure equal to 50% of p_y .

SUMMARY AND CONCLUSIONS

The present work reported the simulation of the mechanical behavior of mitered steel pipe elbows, using rigorous numerical (finite element) tools. Two 90-degree elbows have been examined, with diameter-to-thickness ratio equal to 192 and 240 respectively, considering two types of analyses: (a) elastic analysis for determining flexibility and stress concentration and (b) elastic-plastic analysis for calculating ultimate strength and identifying the corresponding failure mode. Comparison with the response of a “fictitious smooth” bend is also conducted.

Numerical results show that the corners at the connections between adjacent parts of the mitered elbow have a decisive influence on the development of local stresses in the elbow,

affecting the structural response and the ultimate capacity of the bend. Furthermore, the values of flexibility and stress intensity factors, calculated from the relevant ASME provisions, are in several cases rather non-conservative predictions of the values computed numerically. The presence of internal pressure plays a significant role on elbow flexibility and its ultimate capacity, and influences the corresponding mode of failure.

The increased bending flexibility and stress intensity of pipe elbows, with respect to straight pipes, should be taken into account in pipeline analysis under ground-induced actions. More specifically, the models used for pipeline stress analysis should account for both those aspects. Furthermore, due to the development of significant stresses at mitered elbows, especially at the corners, it is not recommended to use elbows at the zone where maximum ground-induced action is expected, especially at fault crossings.

It is also noted that the present study refers to “on-air” pipe elbows, without considering soil-pipe interaction. It is expected that the elbows response under structural loading will be influenced by the surrounding soil; its confining effect will decrease elbow ovalization, reducing local stresses and strains.

Finally, the authors believe that further research is necessary, towards better understanding the mechanical behavior of mitered pipe bends, considering bends with different angles (not only 90-degree elbows). This research should be supported by experimental data, mainly for determining the strength and deformation capacity of the welds at the corners.

ACKNOWLEDGEMENTS

Partial funding for this study has been provided by Northwest Pipe Company.

REFERENCES

- American Society of Mechanical Engineers, (2014), *Power Piping*, B31.1, ASME Code for Pressure Piping, New York, NY.
- American Society of Mechanical Engineers, (2014), *Process Piping*, B31.3, ASME Code for Pressure Piping, New York, NY.
- American Society of Mechanical Engineers, (2012), *Pipeline Transportation Systems for Liquids and Slurries*, B31.4, ASME Code for Pressure Piping, New York, NY.
- American Society of Mechanical Engineers, (2014), *Gas Transmission and Distribution Piping Systems*, B31.8, ASME Code for Pressure Piping, New York, NY.
- American Water Works Association (2004), *Steel Pipe – A Guide for Design and Installation*, AWWA Manual M11, Denver, CO, USA.
- American Water Works Association (2012), *Dimensions for Fabricated Steel Water Pipe Fittings*, AWWA C208, Denver, CO, USA.
- Comité Européen de Normalisation, (2002), *Metallic industrial piping - Part 3: Design and calculation*, Standard EN 13480-3, Brussels.
- Gresnigt, A. M., (2002), “Elastic and plastic design of mitered bends”, *12th International Offshore and Polar Engineering Conference*, Kitakyushu, Japan.

- Karamanos, S. A., Koritsa, E., Keil, B. and Card, R. J. (2015), "Analysis and behavior of steel pipe welded lap joints in geohazard areas.", *ASCE Pipelines Conference*, Paper No. 413, Baltimore, Maryland, USA.
- Karamanos, S. A., (2016), "Mechanical Behavior of Steel Pipe Bends; An Overview.", *Journal of Pressure Vessel Technology*, ASME, Invited paper: special issue for the 50th Anniversary of PVPD, in press.
- Lund, L. V. (1996), "Lifeline Utilities Performance in the 17 January 1994 Northridge, California, Earthquake", *Bulletin of the Seismological Society of America*, Vol. 86, No.1B, pp.S350-S361.
- O' Rourke, T. D. and A. Bonneau, (2007), "Lifeline Performance Under Extreme Loading During Earthquakes," *Earthquake Geotechnical Engineering*, K.D. Pitilakis, Ed., Springer, Dordrecht, Netherlands, June, pp. 407-432,
- Rodabaugh, E. C., and George, H. H., (1957), "Effect of internal pressure on the flexibility and stress intensification factors of curved pipe or welding elbows.", *Transactions of the ASME*, Vol. 79, pp. 939-948
- Rodabaugh E. C., (1975), *Review of data on mitre joints in piping to establish maximum angularity for fabrication of girth butt welds*, WRC Bulletin No. 208.
- Vasilikis, D., Karamanos, S. A., Van Es, S. H. J., Gresnigt, A. M. (2014), "Bending Deformation Capacity of Large-Diameter Spiral-Welded Tubes.", *International Pipeline Conference*, IPC2014-33231, Calgary, Alberta, Canada.
- Von Karman, T., (1911), "Uber die Formuenderung dunnwandiger Rohre." [in German], *Zeit. Des Vereines deutscher Ingenieure*, Vol. 55, pp. 1889-1895.
- Wood, J., (2008), "A review of literature for the structural assessment of mitred bends", *International Journal of Pressure Vessels and Piping*, Vol. 85, pp. 275–294